XL CILAMCE
IBERO-LATIN AMERICAN CONGRESS ON COMPUTATIONAL METHODS IN ENGINEERING
NOVEMBER 11-14, 2019
Praiamar Natal Hotel & Convention
Natal, RN-BRAZIL

FLAT-TOP PARTITION OF UNIT IN THE GENERALIZED FINITE ELEMENT METHOD APPLIED TO DYNAMIC ANALYSIS

Ivan Assing da Silva
Roberto Dalledone Machado
Marcos Arndt
Paulo de Oliveira Weinhardt
ivanassing@gmail.com
rdm@ufpr.br
arndt.marcos@gmail.com
paulo_weinhardt@live.com
Programa de Pós-Graduação em Métodos Numéricos em Engenharia - Universidade Federal do Paraná
R. Cel. Francisco H. dos Santos, 210, 81531-980, Curitiba, Paraná, Brazil

Abstract. The Generalized Finite Element Method (GFEM) has presented excellent results in the dynamic analysis, especially in the obtaining of higher frequencies, one advantage compared to the standard Finite Element Method (FEM). An important feature of GFEM is the possibility of expanding the approximation space through the inclusion of non-polynomial enrichment functions, which usually contain a-priori knowledge about the solution of the problem. However, this enrichment process may lead a problem considerably ill-conditioned, limiting its applicability. This paper proposes the use of *flat-top* functions as a Partition of Unit (PU) for the construction of approximation spaces enriched with non-polynomial functions, aiming to improve the conditioning of the problem by reducing the condition number of stiffness and mass matrices. Results are presented for one-dimensional and two-dimensional problems, such as bars and membranes modal analysis, respectively. The condition number of stiffness and mass matrices are evaluated and compared with results obtained by GFEM with approximation spaces constructed with PU linear. Results obtained with the PU *flat-top* shown improvement in the conditioning of the problems, with the reduction of the condition number of stiffness and mass matrices, however with influences in the accuracy of responses.

Keywords: Generalized finite element method, Dynamic analysis, Flat-top partition of unit, Non-polynomial enrichment.

1 Introduction

The generalized finite element method (GFEM) can be viewed as an extension of the standard finite element method (FEM), also known as the extended finite element method (XFEM), that is a Galerkin method based on the partition of unit method (PUM) (Babuška and Melenk [1, 2]). The main proposal of GFEM is to augment the standard FEM approximation space (trial space) incorporating enrichment functions, that may better represent the problem response, through a partition of unit (PU) (Babuška et al. [3], Melenk [4], Duarte and Oden [5,6], Babuška and Melenk [1, 2], Babuška et al. [7], Belytschko and Black [8], Möes et al. [9]).

GFEM has applications in several areas, such as fracture mechanics, flow of biphasic fluids, electromagnetism, problems with high gradients, and in the context of this paper, dynamic analysis of structures (Arndt [10], Torii [11], Torii and Machado [12], Shang [13], Torii et al. [14], Hsu [15], Weinhardt et al. [16], Piedade Neto and Proença [17]). Despite the excellent results presented in solving these problems, the numerical instability associated with the enrichment process is still a limiting factor regarding its applicability and its efficiency. Several studies in recent years have been addressed to the treatment of this problem, mainly in the context of fracture mechanics.

In order to improve the conditioning of the method, Babuška and Banerjee [18, 19] presented a new approach for the construction of enrichment functions, aiming to create a quasi-orthogonal enrichment function space in relation of the standard FEM approximation space. This modification was so-called the stable generalized finite element method (SGFEM). However, Zhang, Babuška and Banerjee [20] showed that for high order polynomial enrichment ($p > 1$) the modification proposed by the SGFEM is not a sufficient condition to ensure proper conditioning of the problem.

Extending the development of SGFEM, Zhang, Babuška and Banerjee [20] presented a new proposal for the construction of the enrichment function space, replacing the standard PU Lagrangean linear (piecewise linear *hat-functions*) by the PU *flat-top*. This modification was called by the authors as high order SGFEM. However, Zhang, Babuška and Banerjee [20] only addressed the analysis for high order polynomial enrichments, not approaching the case of non-polynomial enrichments. In the context of this paper, problems with dynamic nature are commonly represented by non-polynomial functions, e.g. trigonometric functions, exponential functions.

Therefore, this paper proposes to investigate the GFEM with PU *flat-top*, for the construction of approximation spaces enriched with non-polynomial functions, applied in problems in the context of dynamic analysis. Numerical experiments are performed to verify the influences on the conditioning and accuracy of the frequency spectrum, the results obtained with PU *flat-top* and PU piecewise linear are compared.

2 Modal Analysis

Two problems in the context of the dynamic analysis of structures are addressed in this paper: bar uniaxial free vibration (one-dimensional model) and membrane transverse free vibration (two-dimensional model). These problems were solved through modal dynamic analysis in absence of damping to determine natural frequencies and vibration modes.

The application of the standard FEM procedures (Bathe [21], Hughes [22], Zienkiewicz and Taylor [23]) on the dynamic equilibrium equation of the problem, results in the following system of differential equations:

$$\mathbf{M}\ddot{\mathbf{u}} + \mathbf{K}\mathbf{u} = \mathbf{F} \tag{1}$$

where $\mathbf{K}$ is the stiffness matrix, $\mathbf{u}$ is the displacements vector, $\mathbf{M}$ is the mass matrix and $\mathbf{F}$ is the applied forces vector. The natural frequencies and vibration modes can be obtained solving the generalized eigenproblem defined by (Bathe [21], Hughes [22], Zienkiewicz and Taylor [23]):

$$\mathbf{K}\phi = \omega^2 \mathbf{M}\phi \tag{2}$$

where ω are the natural frequencies and ϕ are the vibration modes of the problem.

The matrices $\mathbf{K}$ and $\mathbf{M}$ can be obtained from discretization and approximation by the standard FEM procedures of the boundary value problem (BVP) related to the dynamic equilibrium of the system. Thus, the matrices $\mathbf{K}$ and $\mathbf{M}$ are constructed, respectively, from the contribution of the elementary matrices $\mathbf{k}^e$ and $\mathbf{m}^e$, given by:

$$\mathbf{k}^e = [k_{ij}] = E\int_{\Omega^e} \nabla\Phi_i \cdot \nabla\Phi_j d\Omega^e \tag{3}$$

$$\mathbf{m}^e = [m_{ij}] = \rho\int_{\Omega^e} \Phi_i \Phi_j d\Omega^e \tag{4}$$

where $\mathbf{\Phi}$ is the shape functions vector (basis of approximation space), E is the modulus of elasticity, ρ is the specific mass and Ω^e is the master element domain.

Equations (3) and (4) are applied to solving both two problems considered in this paper, through proper construction of shape functions. The problems considered in this paper have analytical solution as presented as follow.

2.1 Clamped bar

Consider a straight bar of length L and constant cross-sectional area A, clamped at both ends as shown in Fig. 1.

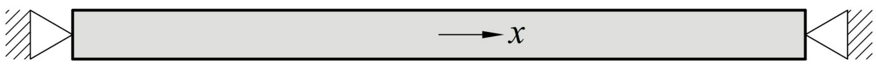

Figure 1. Clamped bar

The analytical solution for natural frequencies can be determined by separating variables (Kreyszig [24]) and is given by:

$$\omega_n = \frac{n\pi}{L}\sqrt{\frac{\rho}{E}} \quad n = 1,2,3\ldots. \tag{5}$$

Considering that the normalized frequency spectrum is independent of the constants, we assumed unit value for all constants: cross-sectional area A, length L, specific mass ρ and modulus of elasticity E. Therefore, the analytical solution can be rewritten as:

$$\omega_n = n\pi \quad n = 1,2,3\ldots. \tag{6}$$

2.2 Clamped square membrane

Consider a square membrane of sides lengths $L_x = L_y$, clamped at all sides as shown in Fig. 2.

The analytical solution for natural frequencies can be determined by separating variables as presented by Kreyszig [24] and is given by:

$$\omega_{mn} = \pi c\sqrt{\frac{m^2}{L_x^2} + \frac{n^2}{L_y^2}} \quad m,n = 1,2,3\ldots. \tag{7}$$

We consider a square membrane unit-side. Considering that the normalized frequency spectrum is independent of constants, again we assumed unit value for all constants: side lengths L_x and L_y, wave propagation velocity $c = \sqrt{E/\rho}$. Therefore, the analytical solution can be rewritten as:

$$\omega_{mn} = \pi\sqrt{m^2 + n^2} \quad m,n = 1,2,3\ldots. \tag{8}$$

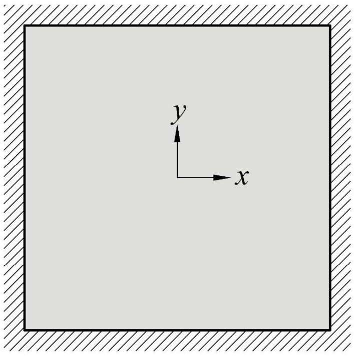

Figure 2. Clamped square membrane

3 Generalized Finite Element Method

GFEM is a Galerkin method based on the partition of unit method (PUM) (Babuška and Melenk [1, 2]), where the standard FEM approximation space is augmented, incorporating new functions, through the product of a PU with enrichment functions (polynomial or non-polynomial), which usually contain a-priori knowledge about the solution of the problem.

The approximate solution u_h^e proposed by GFEM in the master element domain can be written as the sum of two components:

$$u_h^e = u_{FEM}^e + u_{ENR}^e \tag{9}$$

where u_{FEM}^e is the standard FEM component based on the nodal degrees of freedom and u_{ENR}^e is the enrichment component, obtained by multiplying of the PU and the enrichment functions based on the field degrees of freedom. In this sense, the approximate solution on a master element domain is:

$$u_h^e = \sum_{i=1}^{n_n} N_i u_i + \sum_{i=1}^{n_n} \varphi_i \left[\sum_{j=1}^{n_l} \gamma_{ij} a_{ij} + \phi_{ij} b_{ij} \right] \tag{10}$$

where,

- N_i : partition of unit of standard FEM (piecewise linear, *hat-functions*)
- φ_i : partition of unit of enrichment functions
- γ_{ij} , ϕ_{ij} : enrichment functions
- u_i : nodal degrees of freedom
- a_{ij} , b_{ij} : field degrees of freedom, related to enrichment functions
- n_l : number of enrichment levels
- n_n : number of nodes of the finite element

The PU used for enrichment functions is usually the same PU used for the standard FEM component, i.e. $\varphi_i = N_i$. However, the proposal in this paper is to use distinct PUs ($\varphi_i \neq N_i$), considering the PU *flat-top*, as proposed by Zhang, Babuška and Banerjee [20].

The analyzes presented in this paper are performed with two types of partition of unit: PU piecewise linear and PU *flat-top*.

3.1 Partition of unit piecewise linear (*hat-functions*)

The PU piecewise linear, also known as *hat-functions*, is used in the standard FEM component in Eq. (10), and is defined for master element $\xi \in [-1,+1]$ by:

$$N_1 = \frac{1-\xi}{2} \tag{11}$$

$$N_2 = \frac{1+\xi}{2}. \tag{12}$$

In the rest of the paper, we will refer PU piecewise linear as PU linear.

3.2 Partition of unit *flat-top*

The PU *flat-top* used in the enrichment component in Eq. (10) is based on Zhang, Babuška and Banerjee [20], and was rewritten here for a master element $\xi \in [-1,+1]$:

$$\varphi_1(\xi) = \begin{cases} 1 & \xi \in [-1,-\alpha] \\ \left(1-\left(\frac{1}{2}+\frac{\xi}{2\alpha}\right)^l\right)^l & \xi \in [-\alpha,\alpha] \\ 0 & \xi \in [\alpha,+1] \end{cases} \tag{13}$$

$$\varphi_2(\xi) = \begin{cases} 0 & \xi \in [-1,-\alpha] \\ 1-\left(1-\left(\frac{1}{2}+\frac{\xi}{2\alpha}\right)^l\right)^l & \xi \in [-\alpha,\alpha] \\ 1 & \xi \in [\alpha,+1] \end{cases} \tag{14}$$

where $\alpha \in (0,1]$ is the *flat-top* construction parameter and $l \in \mathbb{N}^*$ is the construction parameter that controls the smoothing of the curves between the flat regions. Figures 3 (a) and (b) show, respectively, for the domain $\xi \in [-1,+1]$, the PU *flat-top* with $\alpha = 0.5$ for the cases $l = 1$ and $l = 2$.

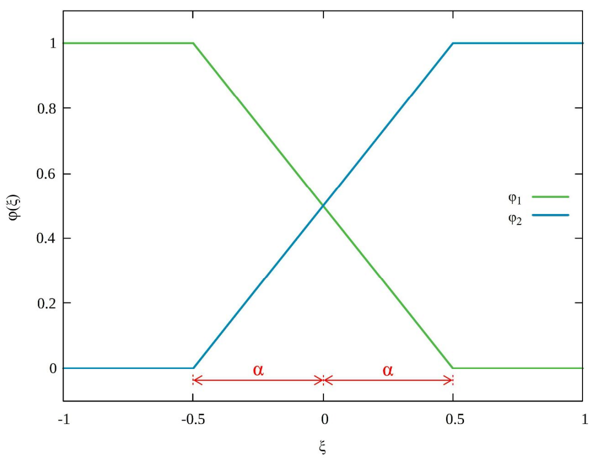

(a)

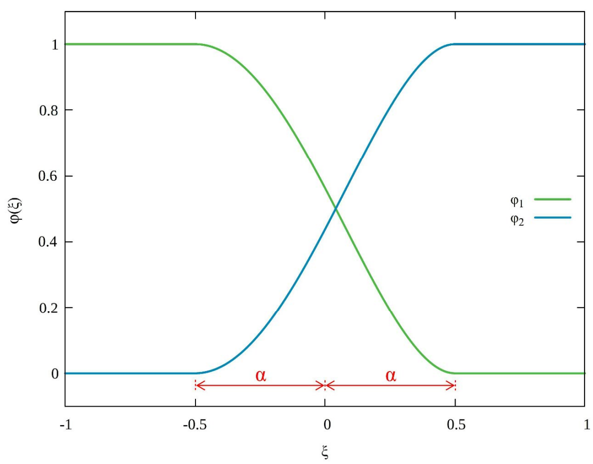

(b)

Figure 3. (a). PU *flat-top*, $\xi \in [-1,+1]$, $\alpha = 0.5$ and $l = 1$. (b). PU *flat-top*, $\xi \in [-1,+1]$, $\alpha = 0.5$ and $l = 2$

The PU linear can be obtained with $\alpha = 1$ and $l = 1$ in Eq. (13) and (14). Practically, the PU linear may be considered as a particular case of PU *flat-top* $\alpha = 1$ and $l = 1$, but not true when $l \neq 1$.

3.3 Trigonometric Enrichment

Enrichment functions may be appropriately selected from a-priori knowledge about the solution of the problem, from analytical solutions or from an estimative about the solution. In the context of dynamic problems, the analytical solutions are commonly represented by harmonic functions. In this sense, trigonometric enrichment has been addressed in several works such as: Arndt [10], Torii [11], Torii and Machado [12], Shang [13,25], Torii et al. [14], Hsu [15], Weinhardt [26] and Weinhardt et al. [16, 27].

The enrichment functions used in this paper are based on the developments of Arndt [10] and Torii [11], and rewritten by Weinhardt [26] for a master element $\xi \in [-1,+1]$:

$$\gamma_{1j} = \sin\left(\beta_j \frac{1+\xi}{2}\right) \tag{15}$$

$$\gamma_{2j} = \sin\left(\beta_j \frac{\xi-1}{2}\right) \tag{16}$$

$$\phi_{1j} = \cos\left(\beta_j \frac{1+\xi}{2}\right) - 1 \tag{17}$$

$$\phi_{2j} = \cos\left(\beta_j \frac{\xi-1}{2}\right) - 1 \tag{18}$$

where β_j is an hierarchical enrichment parameter, originally adopted by Arndt [10] and Torii [11] as:

$$\beta_j = j\pi \quad j = 1,2,3...n_l\,. \tag{19}$$

In this paper, the hierarchical enrichment parameter defined by Eq. (19) is referenced as *standard* β_j.

3.4 Heuristic Modification Stabilization

Weinhardt [26] and Weinhardt et al. [27] presented a modification for the construction rule of the hierarchical enrichment parameter defined by Eq. (19), as a preconditioning strategy for the enrichment functions, which has shown improvement in numerical stability and conditioning. The new stabilized hierarchical enrichment parameter $\bar{\beta}_j$ is defined for a master element $\xi \in [-1,+1]$:

$$\bar{\beta}_j = \left[4(j-1) + \frac{\beta_1}{\pi}\right]\pi \quad j = 1,2,3...n_l\,. \tag{20}$$

In this paper, the hierarchical enrichment parameter defined by Eq. (20) is referenced as *stabilized* $\bar{\beta}_j$.

3.5 One-dimensional element shape functions

The shape functions for the one-dimensional element, with two nodes, are obtained by Eq. (11) and (12), complemented by the multiplication between PU *flat-top* functions, Eq. (13) and (14), with enrichment functions Eq. (15) to (18), properly ordered in accordance with Eq. (10). Figure 4 (a) and (b) show, respectively, for the domain $\xi \in [-1,+1]$, the enriched shape functions with PU linear and PU *flat-top*.

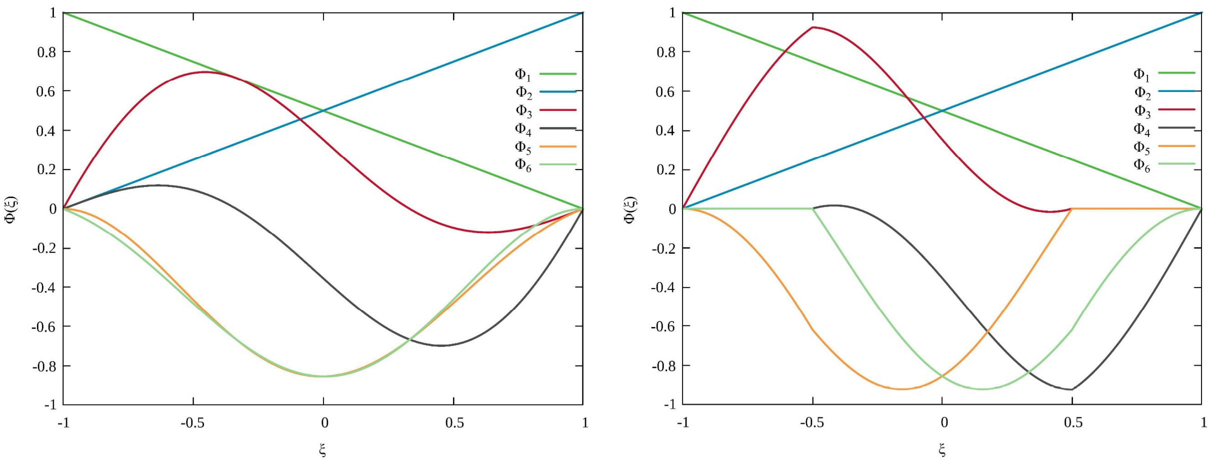

(a) (b)

Figure 4. Trigonometric enriched shape functions. (a). PU linear, $\xi \in [-1,+1]$ and $\beta_1 = 3\pi/2$. (b). PU *flat-top*, $\xi \in [-1,+1]$, $\beta_1 = 3\pi/2, \alpha = 0.5$ and $l = 1$

3.6 Quadrilateral element shape functions

The quadrilateral finite elements, with four nodes, are used for the two-dimensional problem. The shape functions for this element can be obtained by multiplying the shape functions defined for the one-dimensional case. This procedure is described in detail by Solín et al. [28]. The resulting shape functions for the quadrilateral finite element are given by:

$$\Theta_k(\xi,\eta) = \Phi_i(\xi)\Phi_j(\eta) \tag{21}$$

where $\xi \in [-1,+1]$ and $\eta \in [-1,+1]$ define the domain of the quadrilateral master element.

4 Numerical Results

In this section, it is presented the numerical results obtained by GFEM with PU *flat-top* for the problems defined in the section 2.1 and 2.2. The results of PU *flat-top* are verified, with respect to conditioning and accuracy of frequency spectrum, considering the variation of the construction parameters α and l. It is also verified the results of PU *flat-top* applied with hierarchical trigonometric enrichment, according to the hierarchical enrichment parameters *standard* β_j and *stabilized* $\overline{\beta}_j$, defined respectively in Eq. (19) and (20). For the first enrichment parameter, the value $\beta_1 = 3\pi/2$ is adopted due to the good results presented in other works, e.g. Torii [11] and Weinhardt [25], this value is considered for all results presented in this paper.

The Gauss-Legendre quadrature is applied to numerically integrate the stiffness and mass elementary matrices, defined respectively in Eq. (3) and (4). The integration domain is splitted in subdomains according the construction intervals of *flat-top* functions, defined in Eq. (13) and (14). Thus, three subdomains for the unidimensional case and nine subdomains for the bidimensional case. The optimized number of integration points is determined in execution time, according to the complexity of the shape functions employed.

The condition numbers of the stiffness matrix $\kappa(\mathbf{K})$ and mass matrix $\kappa(\mathbf{M})$ are adopted as a measure of the conditioning assessment, knowing that a smaller condition number represents better conditioning (Petroli et al. [29]). The condition number κ for a square matrix is given by (Anderson et al. [30]):

$$\kappa_p(\mathbf{K}) = \|\mathbf{K}\|_p \|\mathbf{K}^{-1}\|_p \tag{22}$$

$$\kappa_p(\mathbf{M}) = \|\mathbf{M}\|_p \|\mathbf{M}^{-1}\|_p \tag{23}$$

where p defines the matrix norm $\|\cdot\|_p$. In this paper the condition numbers are determined by one-norm ($p=1$), that are equivalent to the determined by infinity-norm ($p=\infty$) due stiffness and mass matrices are both symmetric by construction, Hermitian and positive definite matrices (Petroli et al. [29], Weinhardt [26]). Numerically, the condition numbers were determined from the reciprocal of the condition number using the routine DPOCON in LAPACK (Anderson et al. [30]), that apply the Hager's algorithm to estimative the one-norm of the inverse matrix, as proposed by Higham [31].

The approximated natural frequencies are determined from the generalized eigenproblem defined in Eq. (2), that is solved by the divide-and-conquer algorithm through the routine DSYGVD in LAPACK (Anderson et al. [30]).

Results for condition numbers are presented in *log* graphs. The frequency spectra shown approximated frequencies normalized by analytical solution (ω_h/ω) and the degrees of freedom normalized by the total number of degrees of freedom (n/N). All results shown in the graphs are dimensionless.

4.1 Clamped bar (one-dimensional case)

The clamped bar problem defined in section 2.1 is discretized by a uniform mesh with 100 finite elements with length $h=1/100$. The straight bar is clamped at both ends, with length $L=1$, constant cross-sectional area $A=1$, specific mass $\rho=1$ and modulus of elasticity $E=1$. The analytical solution according these considerations is presented by Eq. (6). The problem is solved through modal analysis, with the application of GFEM with PU *flat-top* and PU linear, considering the trigonometric enrichment, the results are presented as follow.

Influence of α parameter. Figures 5 and 6 show results with respect to the influence of the α parameter defined in section 3.2 (PU *flat-top*) on conditioning and frequency spectrum. In this example, only one trigonometric enrichment level ($n_l=1$) is considered.

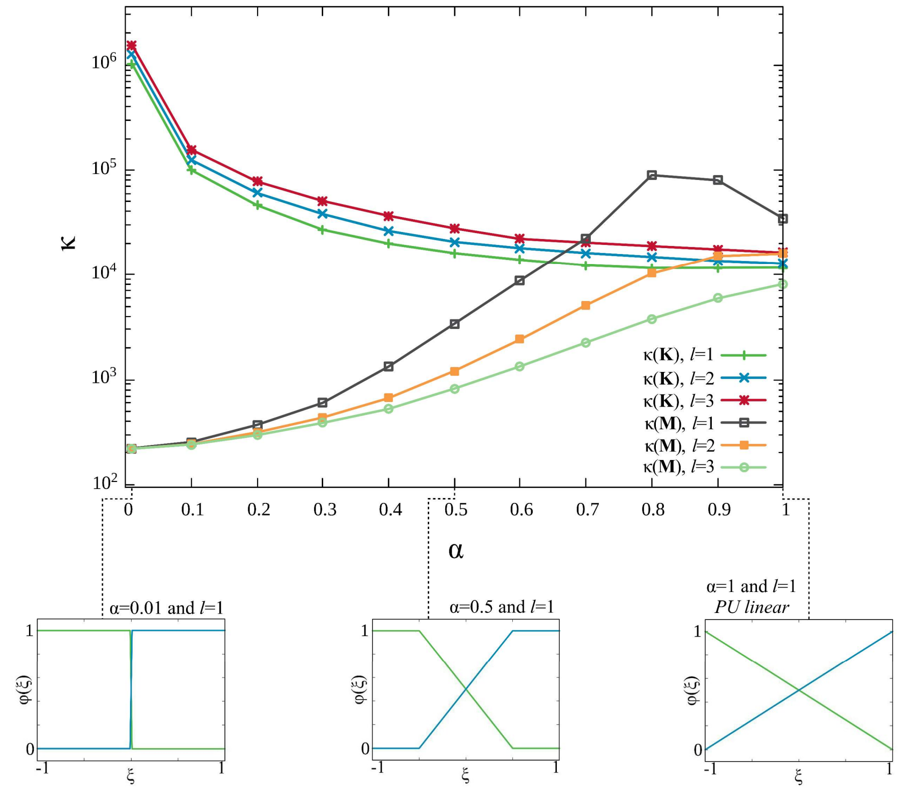

Figure 5. Condition number of the stiffness and mass matrices, $n_l=1$, $\alpha=\{0.01, 0.1, 0.2, 0.3, 0.4, 0.5, 0.6, 0.7, 0.8, 0.9, 1\}$ and $l=1,2,3$.

Figure 5 shows that PU *flat-top* improves in the condition number of the mass matrix, except for $l=1$ when $0.7<\alpha<1$, however, there is an increase of the condition number of the stiffness matrices. Figure 6 (b) shows that PU *flat-top* causes accuracy loss compared to the reference solution shown in Fig. 6 (d), from $O(10^{-5})$ to $O(10^{-3})$, the same conclusion is obtained for PU *flat-top* smoothed with $l=2$, as shown in Fig 6 (c). At the end of the spectrum shown in Fig. 6 (a), the results obtained with $0.1<\alpha<0.4$ are slightly better than the results obtained with PU linear.

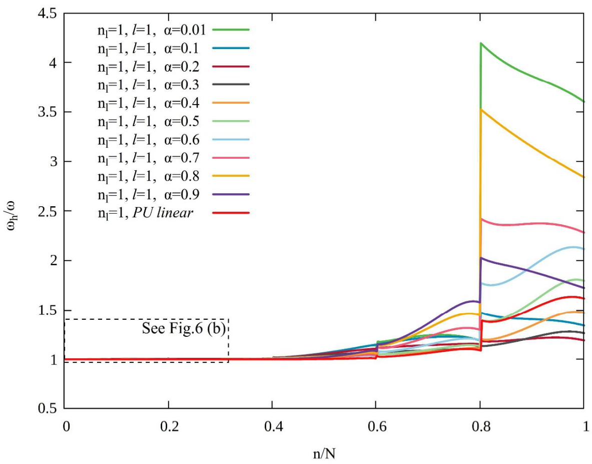

(a)

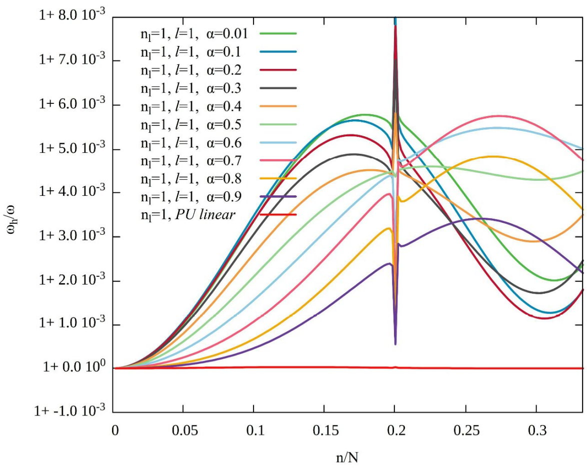

(b)

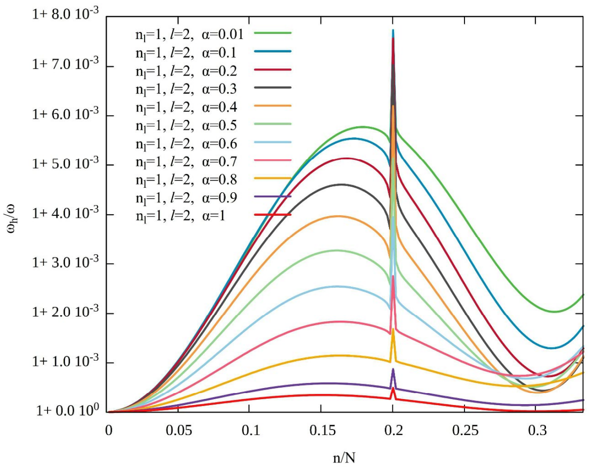

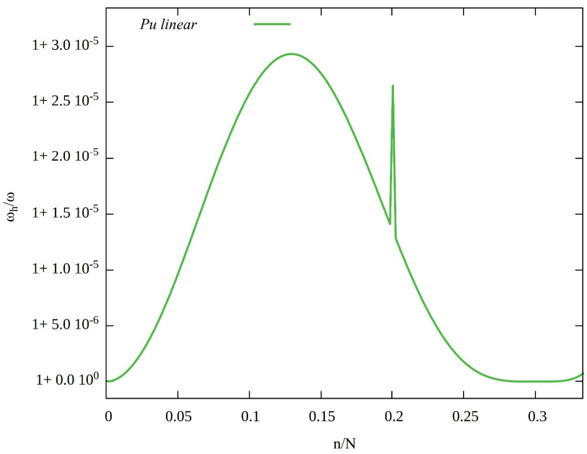

(c) (d)

Figure 6. (a). Frequency spectrum, $n_l=1$, $\alpha=\{0.01,0.1,0.2,...,0.9,1\}$ and $l=1$ (b). Partial spectrum (1/3) of (a). (c). Frequency spectrum (partial 1/3), $n_l=1$, $\alpha=\{0.01,0.1,0.2,...,0.9,1\}$ and $l=2$. (d) Frequency spectrum, GFEM PU linear and $n_l=1$

Influence of l parameter (smoothing of flat-top curve). Figure 7 shows the influence of the parameter that controls the smoothing of the curves between the flat regions.

Figures 7 (a) and (b) show that results obtained with *flat-top* functions with $l=2$ present better accuracy than the results with $l=1$. In addition, *flat-top* functions with $l=2$ has smaller condition number for mass matrix as shown in Fig. 5. Note that in Zhang, Babuška and Banerjee [20] it was considered only $l=1$ for the numerical experiments. The results presented here indicate that it is possible to obtain better conditioning and accuracy for other l values, suggesting further investigation about this parameter.

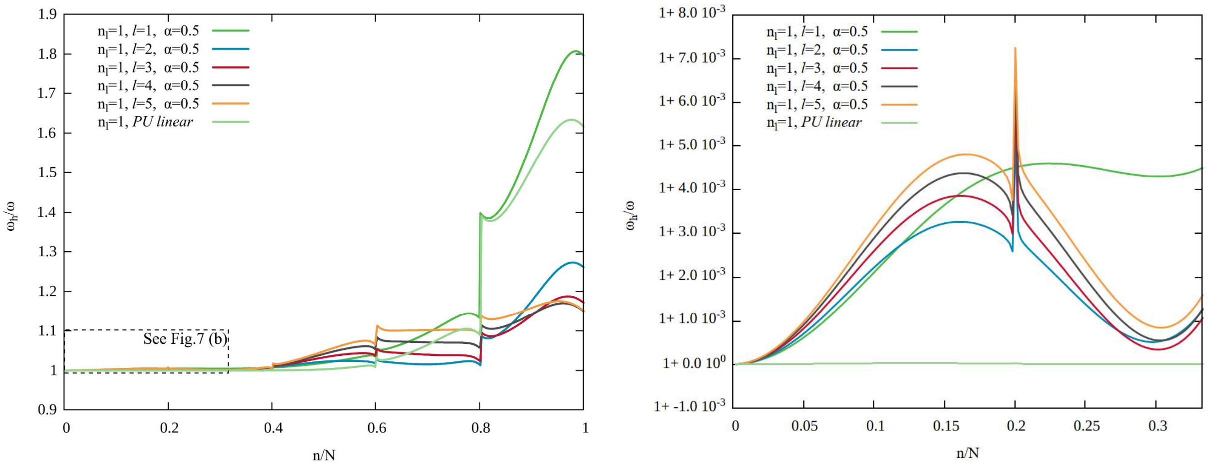

(a) (b)

Figure 7. (a). Frequency spectrum, $n_l = 1$, $\alpha = 0.5$, $l = 1,...,5$. (b). Partial spectrum (1/3) of (a).

Influence on hierarchical trigonometric enrichment. Figures 8, 9 and 10 show the results obtained with hierarchical enrichment parameters *standard* β_j and *stabilized* $\overline{\beta}_j$.

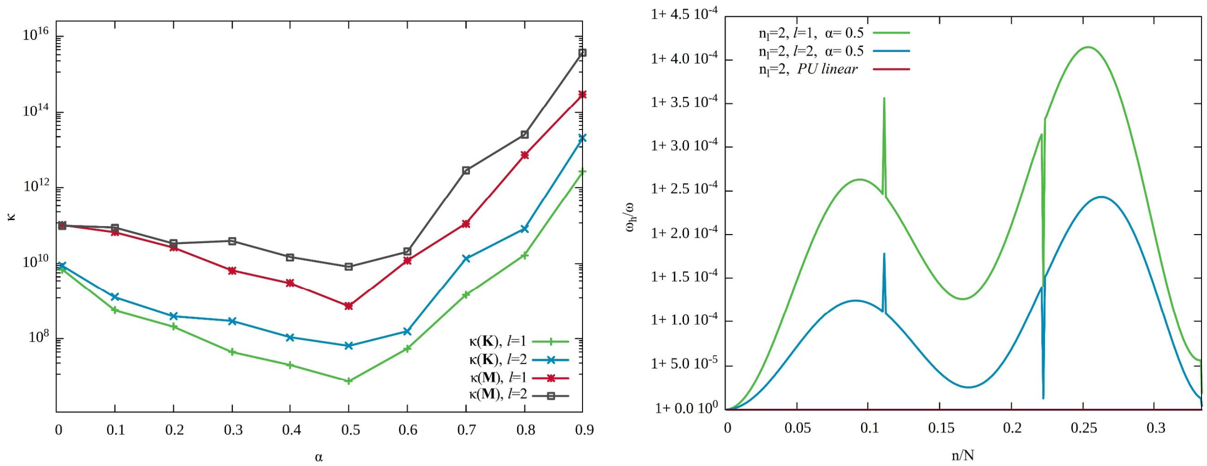

(a) (b)

Figure 8. (a). Condition number of the mass and stiffness matrices, *standard* β_j, $n_l = 5$, $\alpha = \{0.01, 0.1, 0.2, ..., 0.9\}$ and $l = 1,2$. (b) Partial frequency spectrum (1/3), *standard* β_j, $n_l = 2$, $\alpha = 0.5$ and $l = 1,2$.

In the case of hierarchical trigonometric enrichment with *standard* β_j, PU *flat-top* reduces the condition number in both mass and stiffness matrices, as shown in Figs. 8 (a), 9 (a) and (b), with smaller condition numbers obtained with α values close to 0.5. However, there is also accuracy loss in the approximated frequencies, as shown in Fig. 8 (b), from $O(10^{-8})$, as presented by Weinhardt [26], to $O(10^{-4})$.

In the case with *stabilized* $\overline{\beta}_j$, Figs. 10 (a) and (c) show that there is a reduction in the condition number of the mass matrix, however with accuracy loss as shown in Fig. 10 (b). For the stiffness matrix, there is no significant change in the condition number, as shown in Figs. 10 (a) and (d).

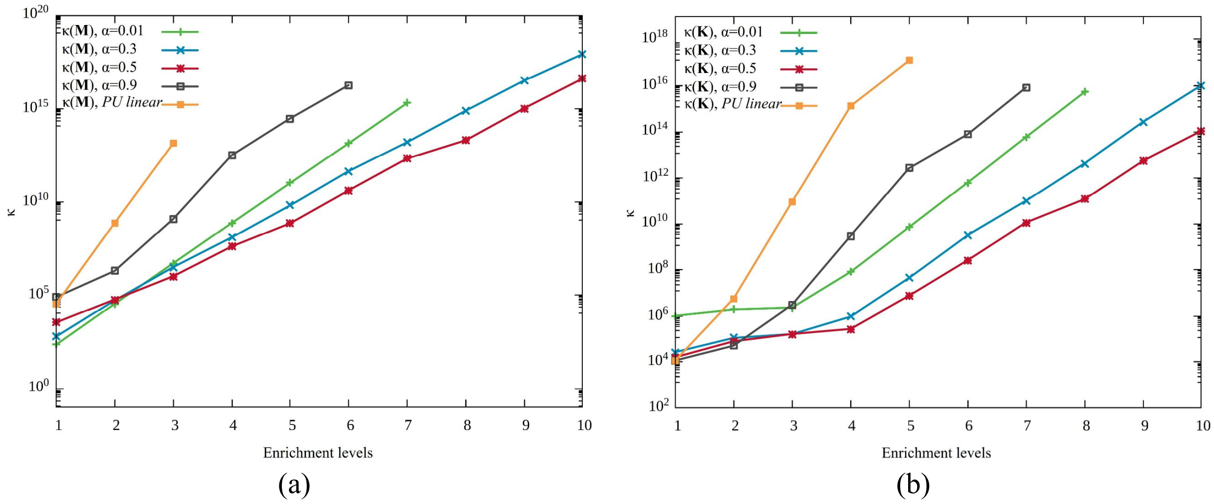

Figure 9. (a). Condition number of the mass matrix, *standard* β_j, $l=1$, $n_l=1,...,10$ and $\alpha=\{0.01,0.3,0.5,0.9,1\}$. (b). Condition number of the stiffness matrix, *standard* β_j, $l=1$, $n_l=1,...,10$ and $\alpha=\{0.01,0.3,0.5,0.9,1\}$

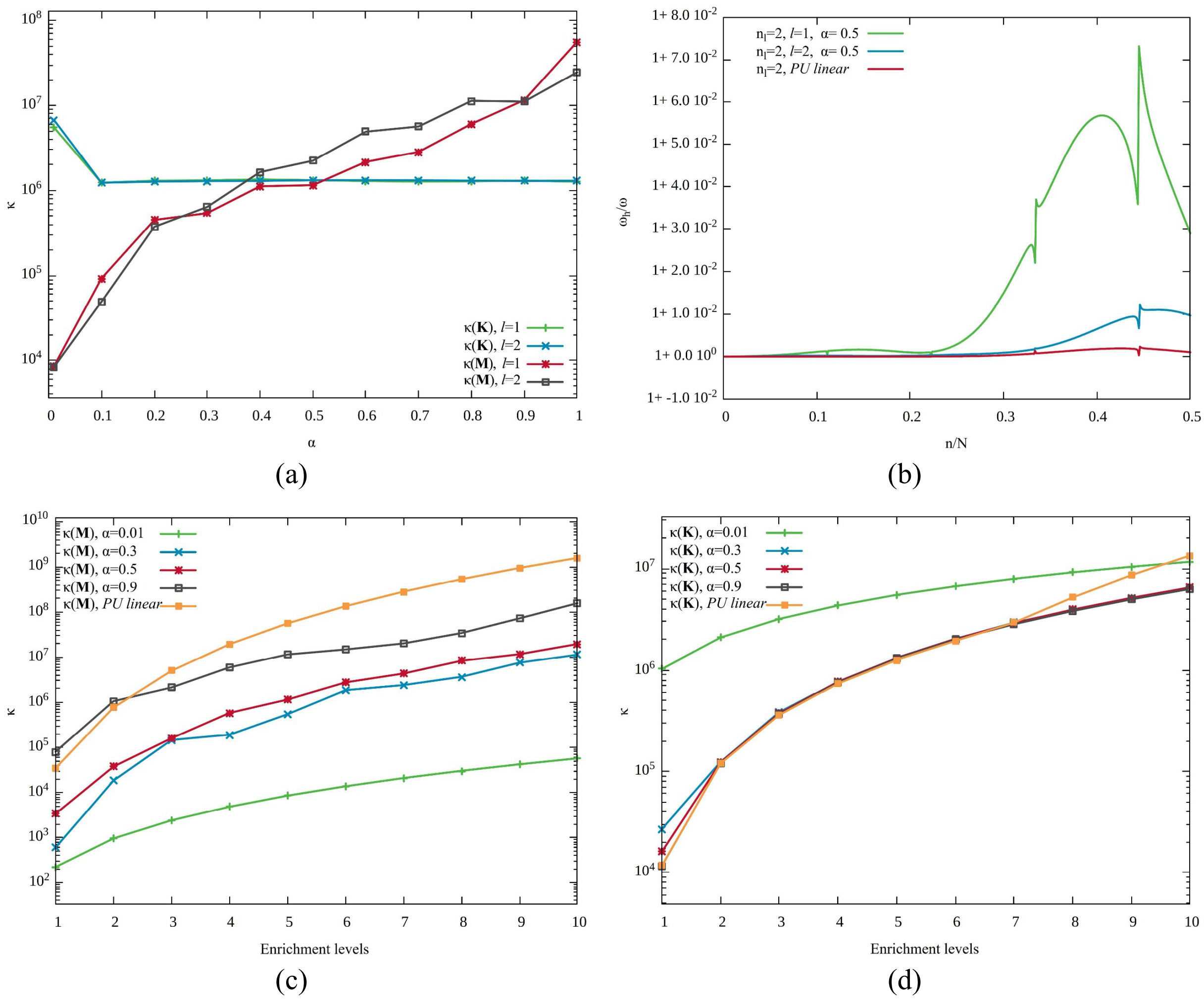

Figure 10. (a). Condition number of the mass and stiffness matrices, *stabilized* $\bar{\beta}_j$, $n_l=5$, $\alpha=\{0.01,0.1,0.2,...,0.9,1\}$ and $l=1,2$. (b) Partial frequency spectrum (1/2), *stabilized* $\bar{\beta}_j$, $n_l=5$, $\alpha=0.5$ and $l=1,2$. (c). Condition number of the mass matrix, *stabilized* $\bar{\beta}_j$, $l=1$, $n_l=1,...,10$ and $\alpha=\{0.01,0.3,0.5,0.9,1\}$. (d). Condition number of the stiffness matrix, *stabilized* $\bar{\beta}_j$, $l=1$, $n_l=1,...,10$ and $\alpha=\{0.01,0.3,0.5,0.9,1\}$

4.2 Clamped square membrane (two-dimensional case)

The clamped square membrane problem defined in section 2.1 is discretized by a uniform mesh with 4 quadrilateral finite elements with sides length $h = 1/2$. The square membrane is clamped at all sides, with side lengths $L = 1$ and wave propagation velocity $c = 1$. The analytical solution according these considerations is presented by Eq. (8). The problem is solved through modal analysis, with the application of GFEM with PU *flat-top* and PU linear, considering the trigonometric enrichment. The results are presented as follow.

Influence of α parameter. Figures 11 and 12 show results with respect to the influence of the α parameter on conditioning and frequency spectrum. In this example only one trigonometric enrichment level ($n_l = 1$) is considered.

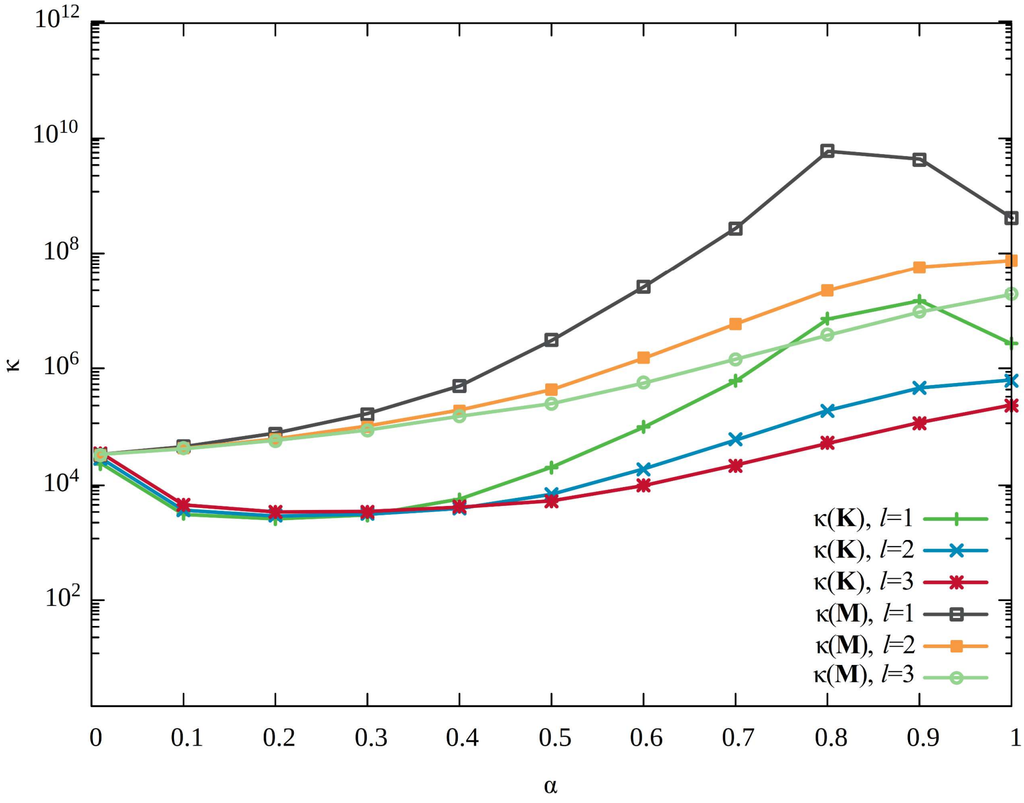

Figure 11. Condition number of the mass and stiffness matrices, $n_l = 1$, $\alpha = \{0.01, 0.1, 0.2, 0.3, 0.4, 0.5, 0.6, 0.7, 0.8, 0.9, 1\}$ and $l = 1,2,3$

In the two-dimensional case with only one enrichment level, PU *flat-top* improves the condition number of the mass matrix, except for $l = 1$ when $0.7 < \alpha < 1$, as shown in Fig. 11, similarly to the results for the one-dimensional case. Also, PU *flat-top* causes accuracy loss when $l = 1$, compared to the reference solution shown in Fig. 12 (d). However, for the case with $l = 2$ and $0.9 < \alpha < 1$ there is accuracy improvement in practically all spectrum, as shown in Figs. 13 (a) and (b), except for the first frequencies.

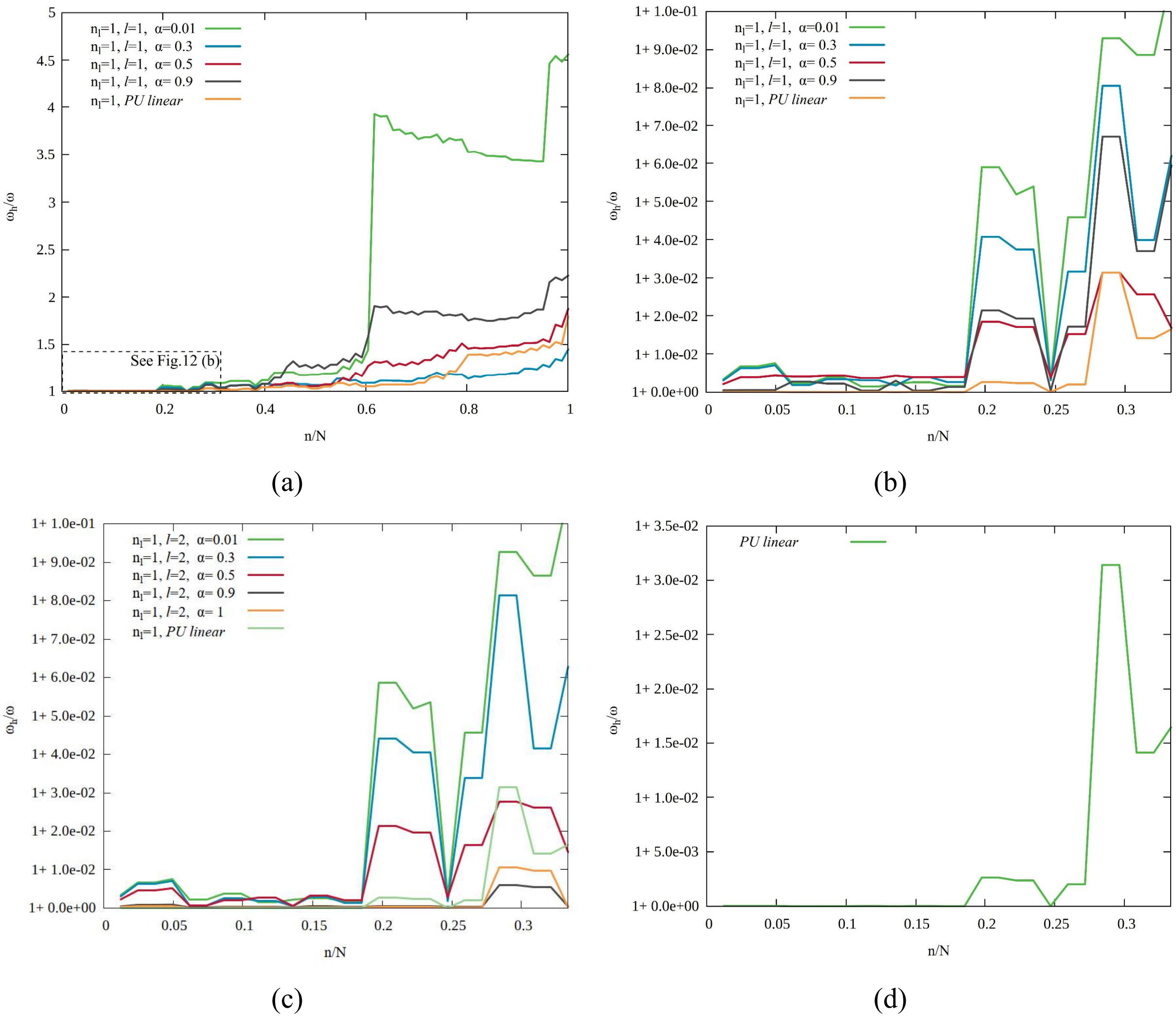

Figure 12. (a). Frequency spectrum, $n_l = 1$, $\alpha = \{0.01, 0.3, 0.5, 0.9, 1\}$ and $l = 1$ (b). Partial spectrum (1/3) of (a). (c). Frequency spectrum (partial 1/3), $n_l = 1$, $\alpha = \{0.01, 0.3, 0.5, 0.9, 1\}$ and $l = 2$. (d) Partial spectrum (1/3), GFEM PU linear and $n_l = 1$

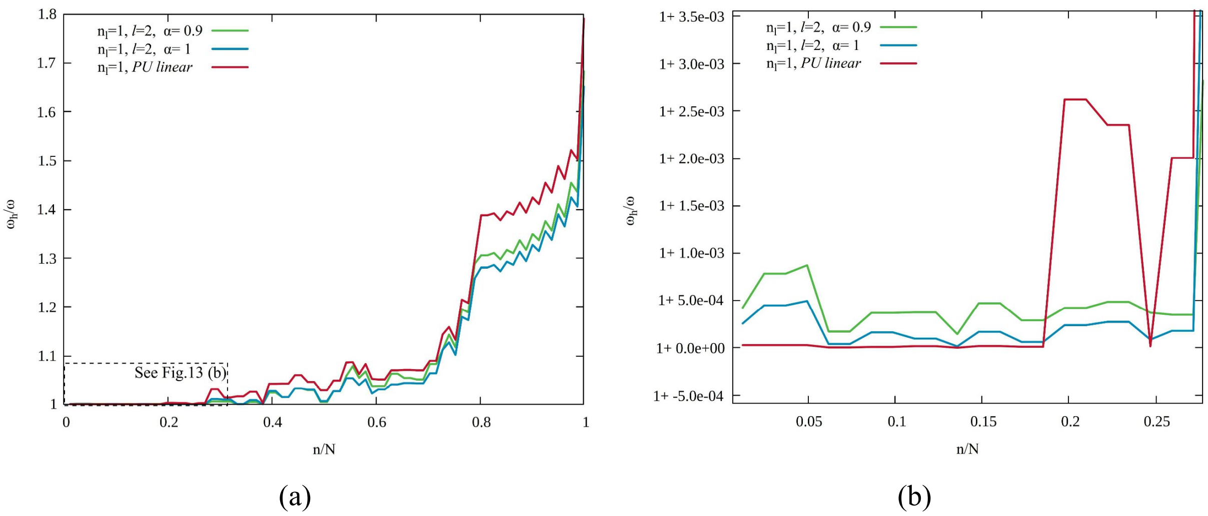

Figure 13. (a). Frequency spectrum, $n_l = 1$, $\alpha = \{0.9, 1\}$ and $l = 2$ (b). Partial spectrum (1/4) of (a).

Influence of l ***parameter (smoothing of flat-top curve).*** Figure 14 shows the influence of the parameter that controls the smoothing of the curves between the flat regions.

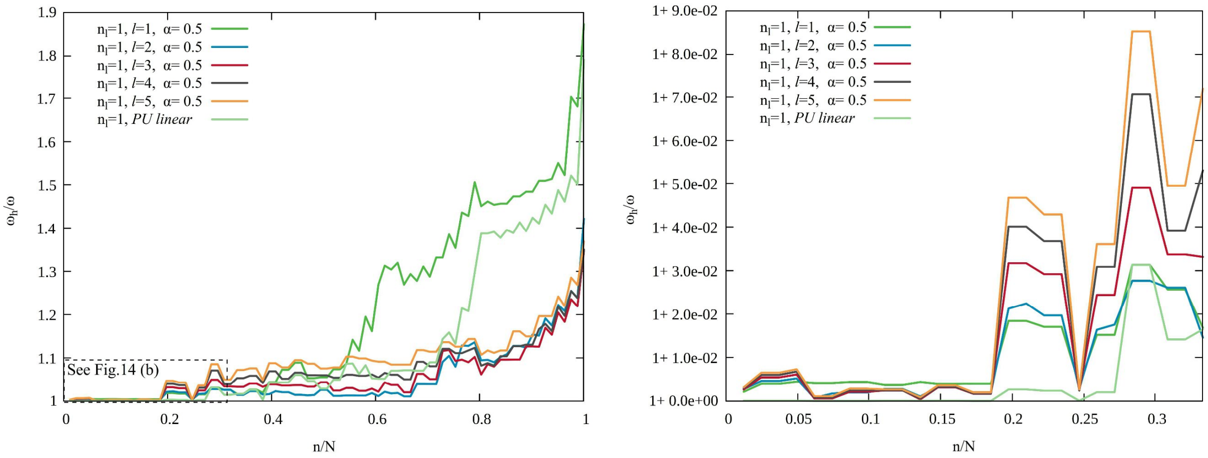

(a) (b)

Figure 14. (a). Frequency spectrum, $n_l = 1$, $\alpha = 0.5$, $l = 1,...,5$ (b). Partial spectrum (1/3) of (a).

As well as in the one-dimensional case, the results obtained by *flat-top* functions with $l = 2$ presented better accuracy than the results with $l = 1$ specially for higher frequencies, as shown in Figs. 14 (a) and (b), also presented smaller condition number for mass and stiffness matrices, as shown in Fig. 11.

Influence on hierarchical trigonometric enrichment. Figures 15 and 16 show the results obtained with hierarchical enrichment parameters *standard* β_j. Figures 17 and 18 show the respective results for *stabilized* $\overline{\beta}_j$.

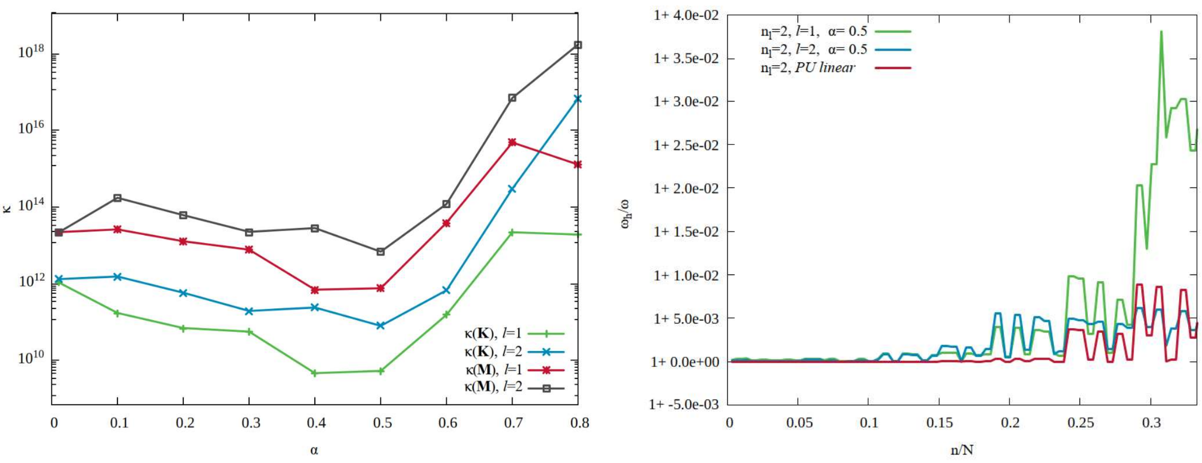

(a) (b)

Figure 15. (a). Condition number of the mass and stiffness matrices, *standard* β_j, $n_l = 3$, $\alpha = \{0.01, 0.1, 0.2, ..., 0.8\}$ and $l = 1,2$. (b) Partial spectrum (1/3), *standard* β_j, $n_l = 2$, $\alpha = 0.5$ and $l = 1,2$.

In the case with *standard* β_j, PU *flat-top* reduces the condition number in both mass and stiffness matrices, as shown in Figs. 15 (a), 16 (a) and (b), with smaller condition numbers obtained with $0.4 < \alpha < 0.5$. However, there is also accuracy loss in the approximated frequencies, as shown in

Fig. 15 (b). The conclusions about the results obtained for the two-dimensional case are similar to the conclusions for the one-dimensional case.

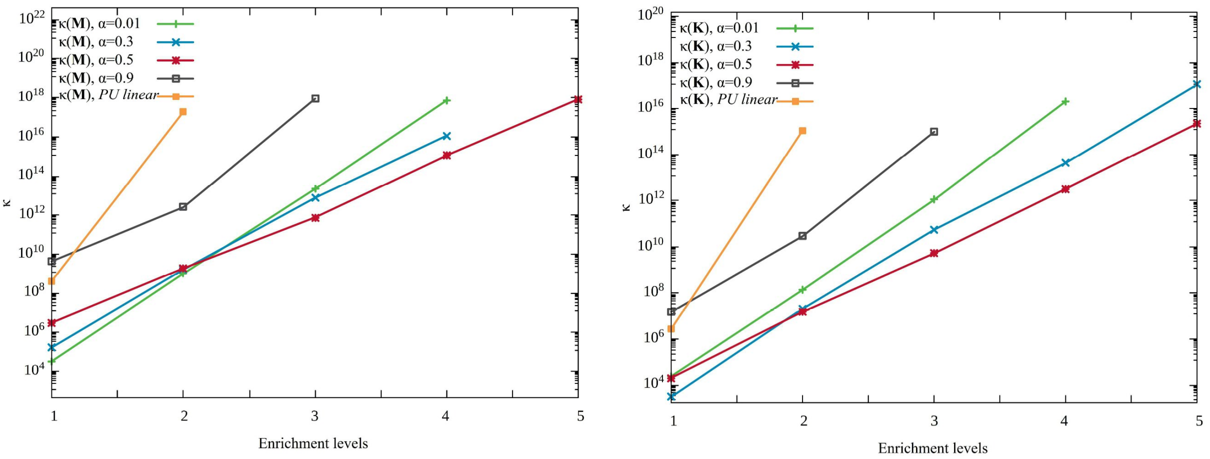

(a) (b)

Figure 16. (a). Condition number of the mass matrix, *standard* β_j, $l=1$, $n_l=1,...,5$ and $\alpha=\{0.01,0.3,0.5,0.9,1\}$. (b). Condition number of the stiffness matrix, *standard* β_j, $l=1$, $n_l=1,...,5$ and $\alpha=\{0.01,0.3,0.5,0.9,1\}$

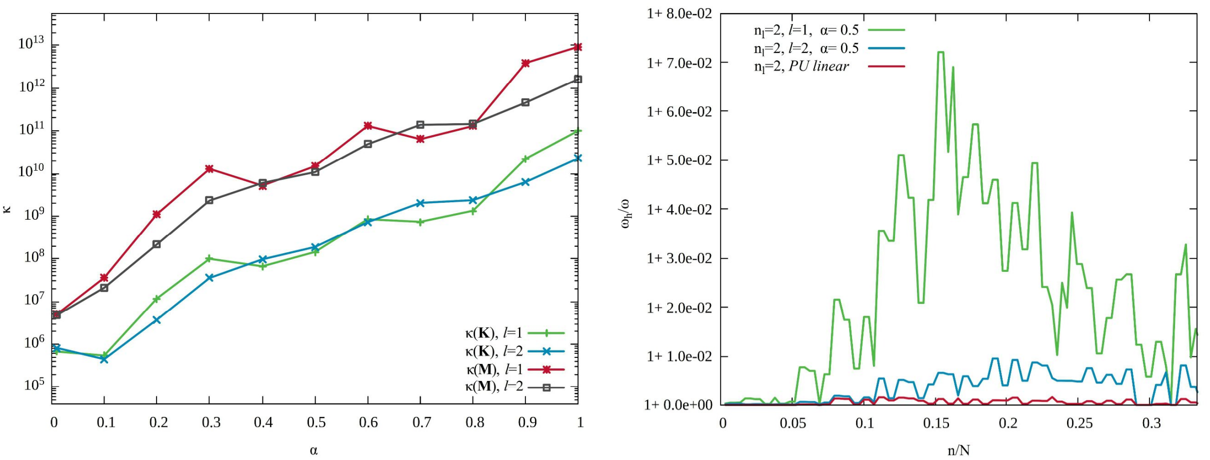

(a) (b)

Figure 17. (a). Condition number of the mass and stiffness matrices, *stabilized* $\overline{\beta}_j$, $n_l=3$, $\alpha=\{0.01,0.1,0.2,...,0.9,1\}$ and $l=1,2$. (b) Partial spectrum (1/3), *stabilized* $\overline{\beta}_j$, $n_l=2$, $\alpha=0.5$ and $l=1,2$.

In the case with *stabilized* $\overline{\beta}_j$, Figs. 17 (a), 18 (a) and (b) show that there is a reduction in the condition number of the both mass and stiffness matrices, when in the one-dimensional case there was not significant improvement of condition number of stiffness matrices. Also, there is accuracy loss as shown in Fig. 17 (b), from $O(10^{-3})$ to $O(10^{-2})$.

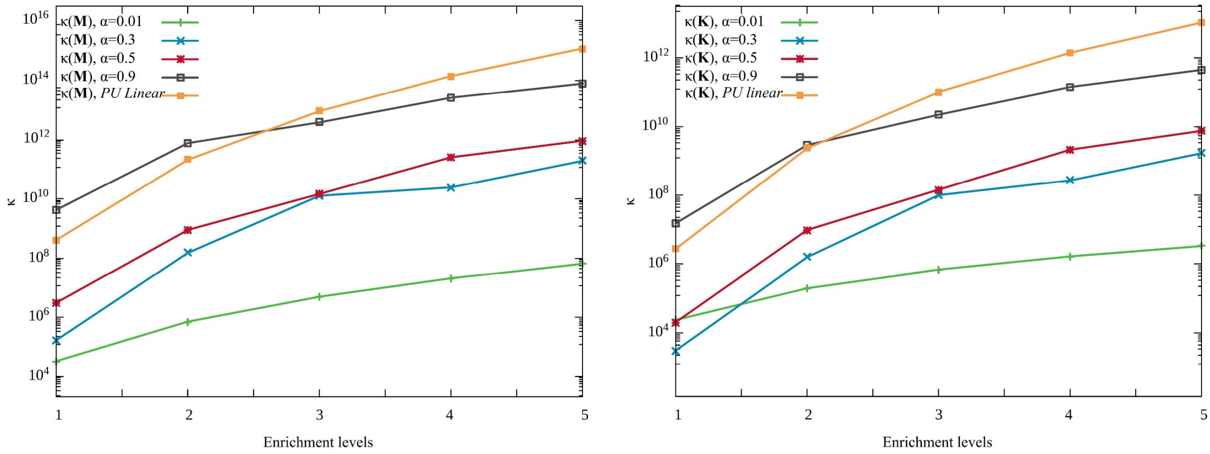

(a) (b)

Figure 18 (a). Condition number of the mass matrix, *stabilized* $\overline{\beta}_j$, $l=1$, $n_l=1,...,5$ and $\alpha=\{0.01,0.3,0.5,0.9,1\}$. (b). Condition number of the stiffness matrix, *stabilized* $\overline{\beta}_j$, $l=1$, $n_l=1,...,5$ and $\alpha=\{0.01,0.3,0.5,0.9,1\}$

5 Conclusions

In this paper, we have addressed the GFEM with PU *flat-top* applied to the dynamic analysis, with non-polynomial enrichments, in order to verify the method conditioning and influences in the accuracy of the responses. The PU *flat-top* was applied to construct approximation spaces hierarchically enriched with trigonometric functions, based on the proposals of Arndt [10], Torii [11] and Weinhardt [26]. GFEM was applied to solve two classical dynamics problems by modal analysis: one-dimensional bar and two-dimensional membrane.

In most cases, the results presented show that PU *flat-top* improved the problem conditioning, with the reduction of the condition number of stiffness and mass matrices, especially for cases with hierarchical enrichment, in both application of enrichment parameters: *standard* β_j and *stabilized* $\overline{\beta}_j$. In cases with the hierarchical stabilized enrichment, the stabilization observed by Weinhardt [26] was maintained and improved with the reduction of magnitude order of the condition number. However, the results with PU *flat-top* were less accurate than the results from PU linear, especially at lower frequencies. Results of conditioning and accuracy were significantly altered by the construction parameters of the *flat-top* functions (α and l), for some cases there was improvement in conditioning and also in accuracy (e.g. $l=2$ and $0.9<\alpha<1$).

References

[1] Babuška, I.; Melenk, J.M.: The partition of unity finite element method. *International Journal for Numerical Methods in Engineering* 40, 727–758, 1997.
[2] Melenk, J.M.; Babuška, I.: The partition of unity finite element method: theory and application. *Computer Methods in Applied Mechanics Engineering* 139, 289–314, 1996.
[3] Babuška, I.; Caloz, G.; Osborn, J. E. Special finite element methods for a class of second order elliptic problems with rough coefficients. *SIAM Journal on Numerical Analysis* 31, 945-981, 1994.
[4] Melenk, J. M. *On generalized finite element methods.* PhD Dissertation. The University of Maryland, 1995.
[5] Duarte, C. A.; Oden, J. T. An h-p adaptive method using clouds. *Computer Methods in Applied Mechanics and Engineering* 139, 237–262, 1996.
[6] Duarte, C. A.; Oden, J. T. Hp clouds and hp meshless method. *Numerical Methods for Partial Differential Equations* 12, 673–706, 1996.

[7] Babuška, I.; Banerjee, U.; Osborn, J.E. Generalized finite element methods: main ideas, results, and perspective. Technical Report No. 04-08, *TICAM*, University of Texas at Austin, Austin, 2004.
[8] Belytschko, T.; Black, T. Elastic crack growth in finite elements with minimal remeshing. *International Journal for Numerical Methods in Engineering* 45, 601– 620, 1999.
[9] Möes, N.; Dolbow, J.; Belytschko, T. A Finite Element Method for crack growth without remeshing. *International Journal for Numerical Methods in Engineering* 46, 131-150, 1999
[10] Arndt, M. *The Generalized Finite Element Method applied to free vibration analysis of framed structures.* Thesis, Federal University of Paraná, Brazil, 2009.
[11] Torii, A. J. *Dynamic analysis of structures with the Generalized Finite Element Method.* Thesis, Federal University of Paraná, 2012.
[12] Torii, A. J.; Machado, R. D. Structural dynamic analysis for time response of bars and trusses using the generalized finite element method. *Latin American Journal of Solids and Structures* 9, 1–31, 2012.
[13] Shang, Y. H. *Dynamic elastoplastic analysis of solids mechanics problems via enriched finite element methods.* Thesis, Pontifical Catholic University of Paraná, 2014.
[14] Torii, A. J.; Machado, R. D.; Arndt, M. GFEM for modal analysis of 2D wave equation. *Engineering Computations* 32, 1779–1801, 2016.
[15] Hsu, Y. S. Enriched Finite Element Methods for Timoshenko beam free vibration analysis. *Applied Mathematical Modelling* 40, 7012-7033, 2016.
[16] Weinhardt, P. O.; Arndt, M.; Machado, R. D. GFEM stabilization techniques applied to transient dynamic analysis. *Revista Interdisciplinar De Pesquisa Em Engenharia* 2, 156-170, 2016.
[17] Piedade Neto, D.; Proença, S. P. B. Generalized Finite Element Method in linear and nonlinear structural dynamic analyses. *Engineering Computations* 33, 806-830, 2016.
[18] Babuška I.; Banerjee U. Stable generalized finite element method (SGFEM). Technical Report, Technical Report Ices Report 11-07, *The Institute for Computational Engineering and Sciences*, The University of Texas at Austin, Austin, Texas, USA, 2011.
[19] Babuška, I.; Banerjee, U. Stable Generalized Finite Element Method (SGFEM). Computer *Methods in Applied Mechanics and Engineering* 201-204, 91–111, 2012.
[20] Zhang, Q.; Banerjee, U.; Babuška, I. Higher order stable generalized finite element method. *Numerische Mathematik*, 128, 1–29, 2014.
[21] Bathe, K. J. *Finite element procedures*. Prentice-Hall, 1996.
[22] Hughes, T.J.R. *The Finite Element Method: Linear Static and Dynamic Finite Element Analysis.* Prentice Hall, 1987.
[23] Zienkiewicz, O.C.; Taylor, R.L. *The Finite Element Method.* Butterworth-Heinemann, Oxford, 2000.
[24] Kreyszig, E. Advanced Engineering Mathematics. 10 ed. New York, John Wiley & Sons, 2010.
[25] Shang, Y. H.; Machado, R. D.; Abdalla Filho, J.E.; Arndt, M. Numerical analysis of plane stress free vibration in severely distorted mesh by Generalized Finite Element Method. *European Journal of Mechanics - A/Solids*, 2016.
[26] Weinhardt, P. O. *Study of the Stability of the Generalized Finite Element Method applied to Dynamic Analysis*, Federal University of Paraná, 2016.
[27] Weinhardt, P. O.; Debella, L. B.; Arndt, M.; Machado, R. D. GFEM stabilization techniques applied to dynamic analysis of non-uniform section bars. *Latin American Journal of Solids and Structures,* 15, 2018.
[28] Solín, P.; Segeth, K.; Dolezel, I. *Higher-Order Finite Element Methods.* Boca Raton: Chapman & Hall/CRC, 2004.
[29] Petroli, T.; Arndt, M.; Machado, R. D.; Weinhardt, P. O. Numerical stability of GFEM evaluation for free vibration analysis in trussed structures. *Proceedings of the 6th International Symposium on Solid Mechanics*, 1, 761-775, 2017.
[30] Anderson, E.; Bai, Z.; Bischof, C.; Blackford, S.L.; Demmel, J.W.; Dongarra, J.J.; Croz, J.D.; Greenbaum, A.; Hammarling, S.; McKenney, A.; Sorensen, D.C. LAPACK User's Guide, 3rd ed. *Society for Industrial and Applied Mathematics*, 1999.
[31] Higham N.J. FORTRAN codes for estimating the one-norm of a real or complex matrix, with applications to condition estimation. *ACM Transactions on Mathematical Software*, 14, 381-396, 1988.